NASA TECHNICAL NOTE

NASA TN D-3846

NASA TN D-3846

A NUMERICAL METHOD FOR DETERMINING HEATING RATES FROM THICK-CALORIMETER DATA

by C. W. Stroud

Langley Research Center
Langley Station, Hampton, Va.

NATIONAL AERONAUTICS AND SPACE ADMINISTRATION • WASHINGTON, D. C. • MARCH 1967

A NUMERICAL METHOD FOR DETERMINING HEATING RATES FROM THICK-CALORIMETER DATA

By C. W. Stroud

Langley Research Center
Langley Station, Hampton, Va.

NATIONAL AERONAUTICS AND SPACE ADMINISTRATION

For sale by the Clearinghouse for Federal Scientific and Technical Information
Springfield, Virginia 22151 – CFSTI price $3.00

A NUMERICAL METHOD FOR DETERMINING HEATING RATES FROM THICK-CALORIMETER DATA

By C. W. Stroud
Langley Research Center

SUMMARY

A method is presented for reducing the data from a thick calorimeter to determine the heating rate to the surface of the calorimeter. The technique employed was to obtain a numerical solution to the inverse problem of heat transfer by using a digital computer. The variation of material properties with temperature is considered. Calculations are compared with experimental results obtained in an arc-heated air jet.

INTRODUCTION

In recent years numerous experiments have been conducted to determine the aerodynamic heating rates associated with various flight conditions. When heating rates are low or exposure times are short, thin calorimeters are generally used. For high heating rates or long exposure times a thick calorimeter must be used. The determination of heating rates based on data obtained from a thick calorimeter is a more difficult problem than the determination of these rates from a thin calorimeter. The heating rate to a thick calorimeter, when the temperature history of the front surface is known, can be obtained for constant material properties and an insulated back surface. (See refs. 1 and 2, for example.) However, exact solutions are not available for the more practical case where material properties vary with temperature and arbitrary boundary conditions are used at the back surface.

This paper presents a method for computing the heating rate applied to a thick calorimeter, wherein account is taken of the variation of material properties of the calorimeter with temperature and allowance is made for an arbitrary, unknown back-surface boundary condition. Equations have been programed on a digital computer to determine heating-rate histories from thermocouple readings obtained at known locations within a calorimeter. The method is applied to experimental results obtained in an arc-heated air jet and the computed heating rate is compared with the heating rate obtained from thin-calorimeter data.

SYMBOLS

The units used for the physical quantities defined in this section are given in both the International System of Units (SI) (ref. 3) and in U.S. Customary Units. Appendix A presents factors relating these two systems of units.

$F(x)$	initial temperature distribution
$g_1(t)$	temperature history of thermocouple near front surface, ^{o}K (^{o}R)
$g_2(t)$	temperature history of thermocouple near back surface, ^{o}K (^{o}R)
k	thermal conductivity, watts/meter-^{o}K (Btu/ft-sec-^{o}R)
L	total depth of calorimeter, meters (ft)
L_i	distance of thermocouple from front surface, meters (ft)
L_1	depth of first thermocouple, meters (ft)
L_N	depth of last thermocouple, meters (ft)
N	number of thermocouples
q	heating rate, watts/meter^2 (Btu/ft^2-sec)
T	temperature, ^{o}K (^{o}R)
t	time, seconds
Δt	computational time interval, seconds
V	integer (the number of intervals into which the distance between thermocouples is divided)
x	coordinate normal to the front surface, meters (ft)
x_i	distance between computational stations i and $i - 1$, meters (ft)
x'	some point between the boundaries
ϵ	emissivity of the front surface
$\overline{\rho c}$	volumetric specific heat, joules/meter^3-^{o}K (Btu/ft^3-^{o}R)

σ Stefan-Boltzmann constant, 56.7 nanowatts/meter^2-$^\circ$K^4 (0.476×10^{-12} Btu/ft^2-sec-$^\circ$R^4)

Subscripts:

j station number

r integer

i integer between 1 and N

ϕ front surface

Superscript:

m time index, $t = m(\Delta t)$

STATEMENT OF THE PROBLEM

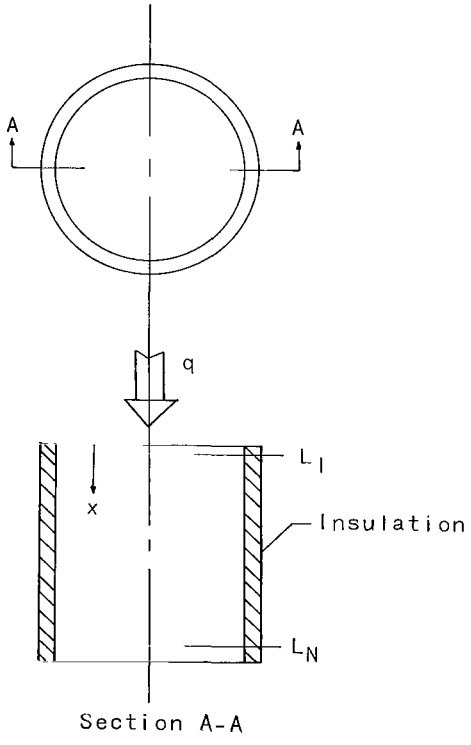

Figure 1.- Sketch of calorimeter.

The problem of heat transfer through a solid may be classified under two general categories. The first category, which might be called the direct problem, consists in obtaining the temperature response of all parts of a solid to a given heat pulse at the surface. In this case the heat pulse and the initial temperature distribution are known and the temperature response of the material is to be determined.

The second category, which might be called the inverse problem of heat transfer, consists in determining the heat pulse to the surface when the temperature response of points within the material is known. The measurement of heat flow with a thick calorimeter falls in the second category. The heat flow through a calorimeter of the configuration shown in figure 1 can be approximated by one-dimensional flow if the thermal conductivity of the surrounding insulation is small compared with the conductivity of the metal calorimeter and if the heating rate does not vary appreciably over the

surface of the calorimeter. With the assumption of one-dimensional heat flow, the heating rate to a surface can be calculated by the following equation. (See ref. 4, for example.)

$$q(t) = \int_0^{x'} \overline{\rho c}(x,t)\frac{\partial T}{\partial t}(x,t)dx - k\frac{\partial T}{\partial x}(t)\bigg|_{x'} + \sigma\epsilon T_\phi{}^4 \tag{1}$$

which is a statement that

Rate of heat in = Rate of heat stored + Rate heat is conducted out
+ Rate heat is rejected by thermal radiation

It is obvious from equation (1) that complete knowledge of the temperature field is needed in order to compute the heating rate directly. For low heating rates or physically thin calorimeters, the rate of change of temperature with time $\frac{\partial T}{\partial t}$ quickly stabilizes and is no longer a function of distance from the surface. If the back surface is assumed to be perfectly insulated and the front surface is not at a high temperature, equation (1) reduces to the simple form:

$$q = L\overline{\rho c}\frac{\partial T}{\partial t} \tag{2}$$

where $\frac{\partial T}{\partial t}$ can be easily measured with a thermocouple located on the back surface. When heating rates are high, that is, when $\left(T_m - T_{initial}\right)\frac{k}{qL}$ is less than about 0.5, the front surface may reach the melting point T_m of the material before the transient phase is completed. Under these conditions, the solution to the thick-calorimeter problem must be obtained. When the thick-calorimeter solution is used, complete knowledge of the temperature history of every point through the thickness of the calorimeter is necessary to solve the inverse problem. Some knowledge of the temperature distribution is obtainable from thermocouples located through the depth of the calorimeter. The procedure followed in the present analysis was to use the temperature-time histories of two points in the material, one point near the surface and the other at some depth in the calorimeter. The solution for the temperature distribution between these points was obtained by utilizing the heat-conduction equation (ref. 5)

$$\frac{\partial}{\partial x}\left(k\frac{\partial T}{\partial x}\right) = \overline{\rho c}\frac{\partial T}{\partial t} \tag{3}$$

subject to the initial condition

$$T(x,0) = F(x) \tag{4a}$$

and the boundary conditions

$$T(L_1,t) = g_1(t) \tag{4b}$$

$$T(L_N,t) = g_2(t) \tag{4c}$$

It must be remembered that the quantities $\overline{\rho c}$ and k in equation (3) are functions of temperature. Furthermore, equation (3) is nonlinear, and numerical methods must be employed for its solution.

NUMERICAL ANALYSIS

The first objective of the numerical procedure is to determine the temperature at all points through the calorimeter as a function of time. Once this information is available, the heating rate to the surface can be computed directly. An explicit formulation of the finite difference is used to obtain a numerical solution of the heat-conduction equation. This method leads to the following finite difference equation (ref. 6):

$$k\left(\frac{T(x+\Delta x,t) + T(x,t)}{2}\right)\left[\frac{T(x+\Delta x,t) - T(x,t)}{\Delta x}\right] - k\left(\frac{T(x,t) + T(x-\Delta x,t)}{2}\right)\left[\frac{T(x,t) - T(x-\Delta x,t)}{\Delta x}\right] = \overline{\rho c}\left(T(x,t)\right)\Delta x\left[\frac{T(x,t+\Delta t) - T(x,t)}{\Delta t}\right] \tag{5}$$

where k and $\overline{\rho c}$ are functions of temperature as indicated by the parentheses. If the temperature distribution is known at time t, then the temperature of point x at time $t + \Delta t$ can be calculated explicitly by equation (5), from the information only at points x, $x - \Delta x$, and $x + \Delta x$ from time t. This approximation can be symbolized as shown in figure 2. The error involved in approximating equation (1) by equation (5) is of the order $\overline{\Delta x}^2$ and Δt. For stability, Δt must satisfy the following inequality (ref. 7):

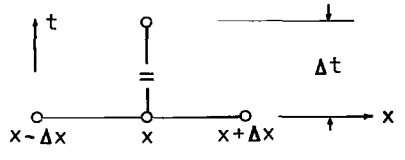

Figure 2.- Representation of finite-difference approximation.

$$\Delta t \leqq \frac{\overline{\rho c}\,(\Delta x)^2}{2k} \tag{6}$$

The value of Δx must be small to preclude any significant truncation errors in the results. A suitably small value can be obtained by decreasing Δx until further changes in its value have no effect on the calculated temperature values.

For convenience, such values of Δx should be selected that the temperatures are calculated at any points at which temperature measurements are made. This can be

accomplished by dividing the distance between successive thermocouple locations into V parts. In figure 3, V is 3. From the same figure it is seen that the thermocouples are located at a depth from the front surface.

$$L_i = \sum_{r=1}^{i} \xi_r \tag{7}$$

where ξ_r is the distance between thermocouples r and r - 1, numbered from the front surface. The boundary thermocouples are located at points i = 1 and i = N and provide the boundary conditions for the solution of equation (5). It should be pointed out that the first thermocouple is not usually located on the front surface and therefore L_1 will have some small value. The distance between each thermocouple is divided into an equal number of finite difference elements. If the boundary thermocouples are the only ones available, all the difference elements will be of equal size. When internal thermocouples are available, the technique used assures that a finite difference station will fall on the exact location of the internal thermocouple. Figure 3 shows that the distance between stations j - 1 and j, designated x_j, is, for a value of j between the limits $(i - 1)V < j \leqq (i)V$,

$$x_j = \frac{\xi_i}{V} \tag{8}$$

where (i)V is the number obtained by multiplying i by V. Equation (5) then takes the form

$$k\left(\frac{T_{j+1} - T_j^m}{x_j}\right) - k\left(\frac{T_j^m - T_{j-1}^m}{x_{j-1}}\right) = (\overline{\rho c})_j^m \left(\frac{T_j^{m+1} - T_j^m}{\Delta t}\right)\left(\frac{x_j + x_{j-1}}{2}\right) \tag{9}$$

where m is the time m(Δt) for integral values of m. The temperatures T_0^m and $T_{(N-1)V}^m$ are obtained from the thermocouples placed at these points. The thermal conductivity is to be evaluated at the average of the two temperatures which it multiplies, and the volumetric specific heat is to be evaluated at T_j^m.

These equations can then be used to calculate the temperature at discrete points between the boundaries for all desired values of time. Additional points can be added to improve accuracy at the expense of computing time.

Once the temperature distribution between the boundary thermocouples has been computed for a given time, other calculations based on these distributions can be made. The temperature of the front surface can now be approximated by using Lagrange's interpolation formula. The interpolation formula used the temperatures of the first 10 finite

difference stations to estimate the temperature of the front surface. Once the temperature of the front surface is obtained, all the necessary information is available to compute the heating rate from equation (1). This calculation was made by the following numerical approximation to equation (1):

$$q^{m+\frac{1}{2}} = \sum_{j=1}^{V(N-1)-1} (\overline{\rho c})_j^m \left(\frac{x_j + x_{j-1}}{2}\right)\left(\frac{T_j^{m+1} - T_j^m}{\Delta t}\right) + (\overline{\rho c})_\phi^m \left(\xi_1 - \frac{x_1}{2}\right)\left(\frac{T_\phi^{m+1} - T_\phi^m}{\Delta t}\right)$$

$$+ k\left[\left(T^{m+1}_{V(N-1)-1} + T^m_{V(N-1)-1}\right) - \left(T^{m+1}_{V(N-1)} + T^m_{V(N-1)}\right)\right]\left(\frac{1}{x_{V(N-1)}}\right) + \sigma\epsilon\left[\left(T_\phi^{m+1}\right)^4 + \left(T_\phi^m\right)^4\right]\frac{\Delta t}{2} \qquad (10)$$

where ϕ represents conditions on the front surface.

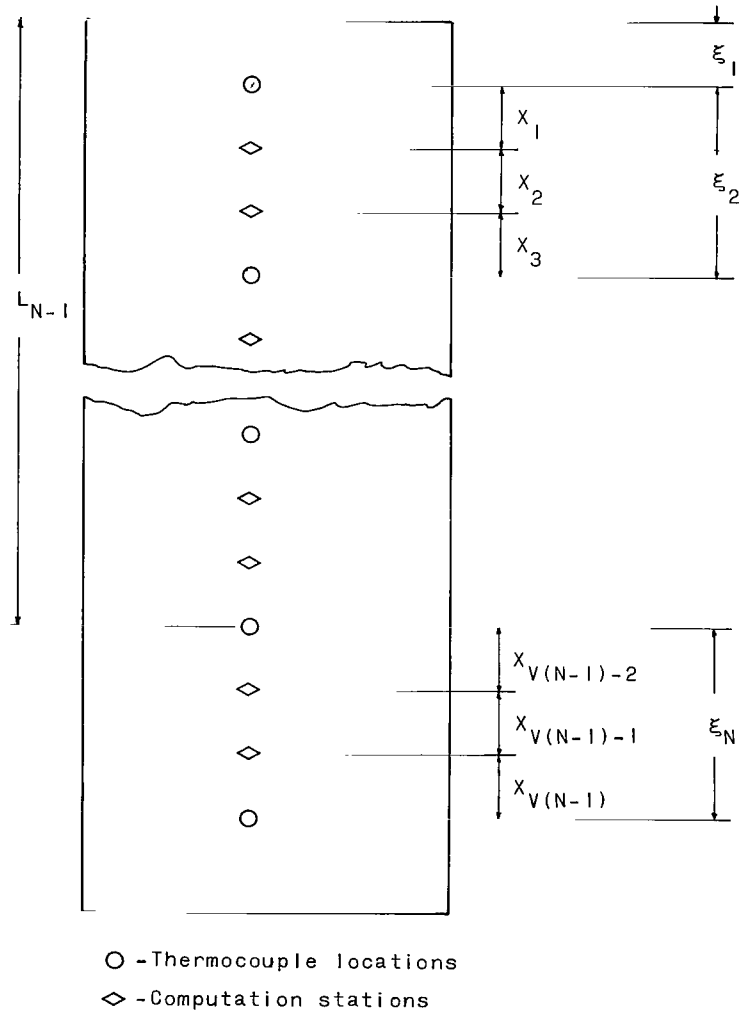

Figure 3.- Location of thermocouples and computation stations in the calorimeter.

It should be pointed out that the solution, as formulated, does not require knowledge of the boundary conditions at the back of the calorimeter in order to calculate correct heating-rate histories. This can be particularly valuable during the latter part of the life of a calorimeter, when the temperature at the back has risen several hundred degrees and an assumption of no heat flow across this boundary may be a poor one. Frequently this period is the more valuable part of the heating history but may be the most inaccurate if a condition of no heat flow across the back surface is an essential part of the solution. The present solution should provide an accurate heating-rate history up until incipient melting of the calorimeter occurs, if the temperatures at the boundaries are known accurately and the conditions of the analysis are met.

ACCURACY OF THE PRESENT INVERSE APPROACH

In order to investigate the errors inherent in such a numerical approach, calculations were made by using information obtained from the direct problem of heat transfer. That is, the heating-rate history to the front surface was given and the temperature response of the boundaries and surface were calculated. The temperature histories of the boundaries and the initial temperature distribution between the boundaries were then used to solve the inverse problem of heat transfer described in the previous section. There is thus available for comparison the correct temperatures and heating rates determined by the direct method.

The direct problems were solved on a computer by an existing finite difference solution which contains provisions for making thermal properties a function of temperature. This program is described in detail in reference 8. The results of the computer solution are referred to hereinafter as direct solutions. Results reported in reference 8 for several linear problems where exact solutions were known indicated the errors in these direct solutions were of the order of 0.1 percent or less.

Direct solutions were obtained for a calorimeter subjected to two typical heat pulses identified as heat pulses A and B. Heat pulse A starts at a high heating-rate level and has a small linear variation with time. Heat pulse B starts at a low heating-rate level and has large changes in heating rate. The material properties used for these computations were those of beryllium taken from reference 9. The temperature responses at the surface and at three points below the surface were calculated. The temperature histories of the three internal points are shown in figure 4 for heat pulse A. Curves (1) and (3) represent the temperatures of the boundary thermocouples and curve number (2) is that of a thermocouple at an internal location.

Six calculated data points, at half-second intervals, were taken from each of these curves and fitted by a fifth-degree least squares polynomial, which in this case goes

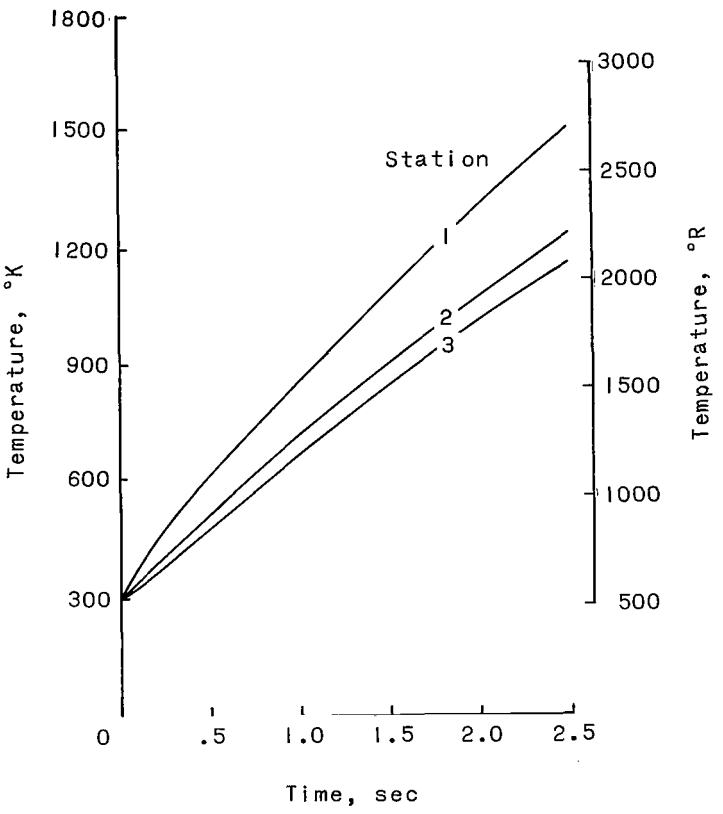

Figure 4.- Calculated temperature response of three locations in the calorimeter to heat pulse A.

through all six points. The coefficients obtained for the polynomials, along with the material property data and the location of the three thermocouple points within the calorimeter, were used as inputs into the inverse program.

The inverse method was used to calculate the temperature history both at the front surface and station (2). From the data generated in these calculations, the heating-rate history of the front surface was determined. The calculated heating-rate history is shown in figure 5 as the solid line, and the input heating rate is the dashed line. The inverse and direct temperatures of the surface and at station (2), as well as the direct and inverse heating rates for the corresponding times are listed in table I. The errors in calculated heating compared to the input heating rate are large during about the first 0.2 second and become relatively small thereafter. These errors are believed to be caused by the failure of the polynomials in the curve fit to reproduce this portion of the temperature history, because they do not seem to be significant after the second point in the curve fit. After this period, the maximum heating-rate error was 4.2 percent, while the average error was only about 1.8 percent.

The computed front-surface temperature, obtained by Lagrange's interpolation formula, is seen in table I to be about 1 percent low throughout the entire range. An error in this direction might be expected, because large changes in the curvature of the temperature profile occur near the surface. This error would cause a deviation of only 0.03 percent in the heating rate determination and is therefore acceptable. The computed temperature at station (2), obtained as a consequence of determining the temperature distribution between stations (1) and (3), shows a maximum error of 5° K (9° R). This error is 1.5 percent of the temperature difference between the boundaries.

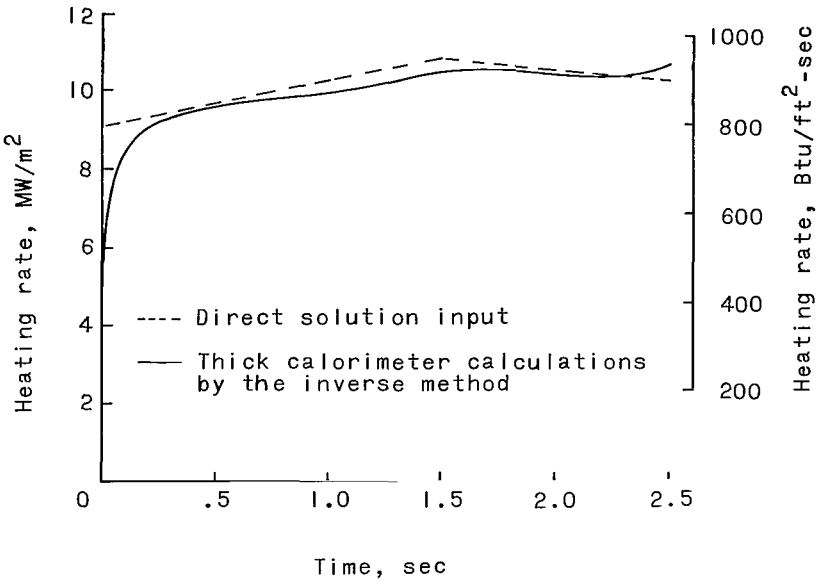

Figure 5.- Comparison of heat pulse A with calculations.

TABLE I.- COMPARISON OF DIRECT AND INVERSE CALCULATIONS OBTAINED FOR HEAT PULSE A

Time, sec	Temperature at front surface				Temperature at station 2				Heating rate, q			
	Direct		Inverse		Direct		Inverse		Direct		Inverse	
	°K	°R	°K	°R	°K	°R	°K	°R	MW/m^2	Btu/ft^2-sec	MW/m^2	Btu/ft^2-sec
0.0	300	540	300	540	300	540	300	540	9.08	800	4.40	388
.5	633	1139	631	1136	510	918	511	920	9.65	850	9.65	850
1.0	869	1565	866	1558	707	1272	710	1278	10.20	900	9.97	878
1.5	1114	2005	1107	1993	896	1612	897	1615	10.76	950	10.44	920
2.0	1348	2426	1337	2407	1074	1934	1076	1936	10.50	925	10.35	912
2.5	1563	2813	1554	2797	1236	2225	1241	2234	10.20	900	10.71	944

The calculated temperature response of three internal points of a calorimeter to heat pulse B are shown in figure 6. For this calculation, the data-taking interval was 0.03125 second. This solution was handled in a manner similar to that used for the other direct solution except for the boundary curves. In order to obtain a good representation of the boundary temperature histories, two curves were spliced together to obtain these temperature histories. The splicing point was taken to be at 0.15625 second. Table II contains a list of inverse and direct temperatures and the corresponding heating rates. The same comments made about the front-surface temperatures for heat pulse A apply here also. The maximum error of the computed temperature at station (2) is 2^{o} K (3^{o} R).

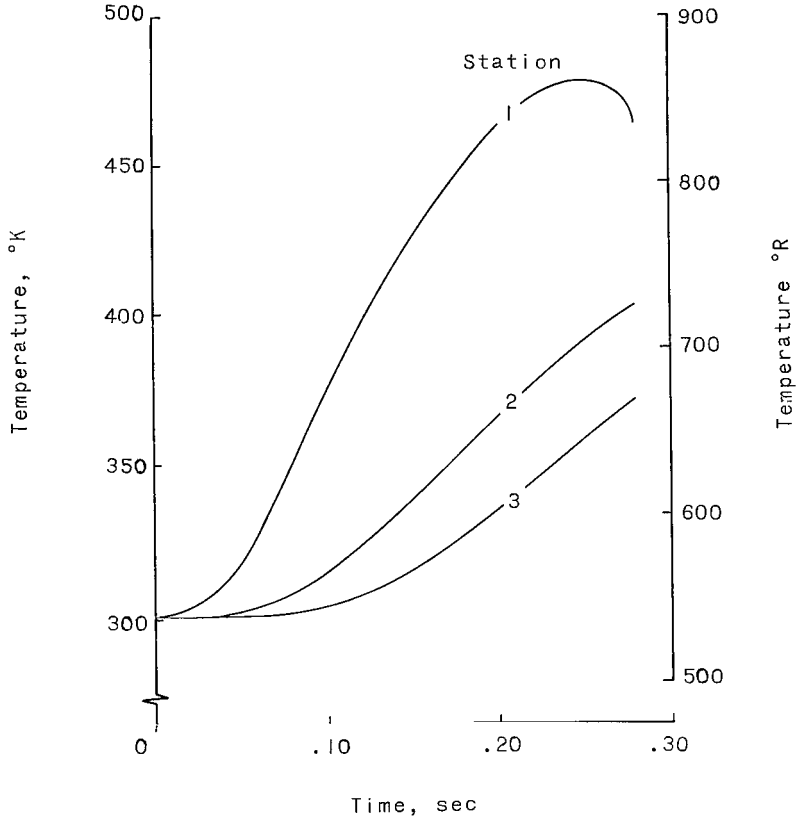

Figure 6.- Calculated temperature response of three locations in the calorimeter to heat pulse B.

TABLE II.- COMPARISON OF DIRECT AND INVERSE CALCULATIONS OBTAINED FOR HEAT PULSE B

Time, sec	Temperature at front surface				Temperature at station 2				Heating rate, q			
	Direct		Inverse		Direct		Inverse		Direct		Inverse	
	°K	°R	°K	°R	°K	°R	°K	°R	MW/m^2	Btu/ft^2-sec	MW/m^2	Btu/ft^2-sec
0.00000	300	540	300	540	300	540	300	540	0	0	0	0
.03125	306	551	306	551	300	540	300	540	1.13	100	1.46	129
.06250	341	613	337	607	303	545	303	546	6.80	600	5.73	505
.09375	386	695	381	685	312	562	313	563	10.20	900	9.20	811
.12500	422	760	416	749	327	589	328	591	10.76	950	10.10	890
.15625	453	815	447	804	343	618	345	621	11.34	1000	11.27	993
.18750	475	855	469	845	361	649	362	652	10.76	950	10.58	932
.21875	493	887	486	874	377	679	379	682	10.20	900	9.65	850
.25000	492	886	487	877	392	706	394	709	6.80	600	7.04	620
.28125	465	837	464	835	404	727	406	730	1.13	100	1.70	150

A comparison of heat pulse B and the calculated heating rate is shown in figure 7 and reasonable agreement was obtained.

Although not exhaustive, the comparisons made between direct and inverse solutions in the problems solved, indicate that the numerical technique used in obtaining the inverse solutions gives reliable results. Those errors that occur are within limits that are tolerable for practical problems.

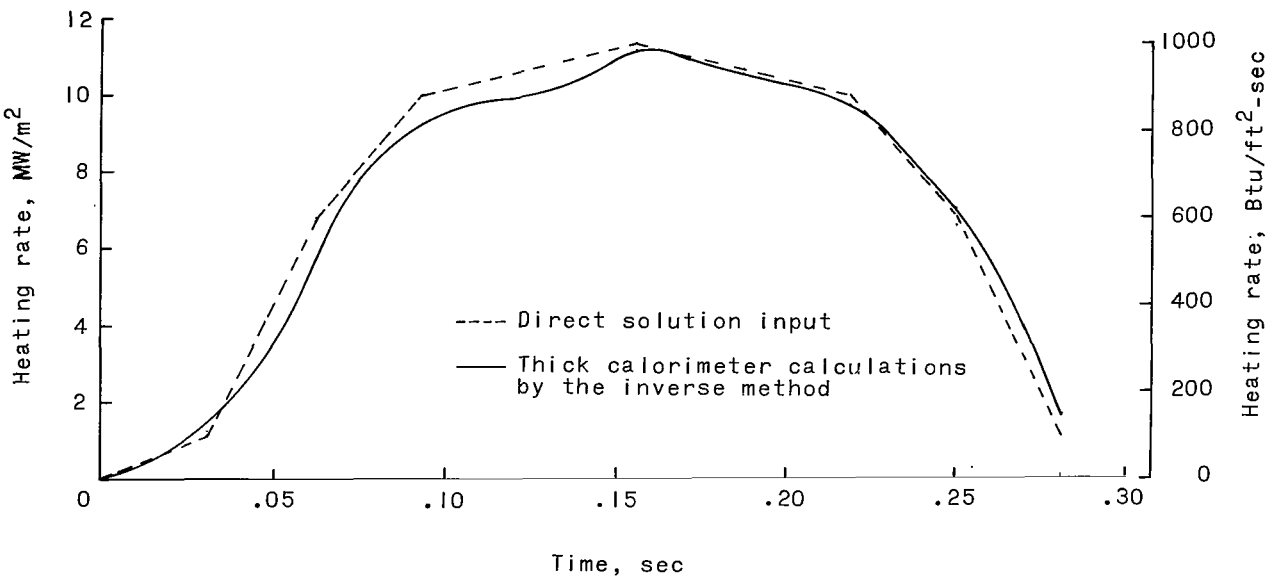

Figure 7.- Comparison of heat pulse B with calculations.

EXPERIMENTAL CORRELATION

In order to obtain experimental data for use in the inverse numerical solution, a thick calorimeter was constructed and subjected to a heat pulse in an arc-heated air jet. Thermocouples placed through the depth of the calorimeter provided the data that were later used as boundary conditions to perform numerical calculations and thus to obtain an inverse solution.

Specimen Description

The calorimeter assembly used to obtain experimental verification of the data-reduction technique is shown in figure 8. The calorimeter was bonded into a holder as shown in the figure. This holder was threaded for mounting directly into the sting of the specimen insertion mechanism. The holder prevents side heating and thereby approximates the boundary conditions of the cylinder in figure 1. The holder was made large

(a) Calorimeter specimen in an insulated holder.
L-65-3388

Figure 8.- Experimental calorimeter specimen.

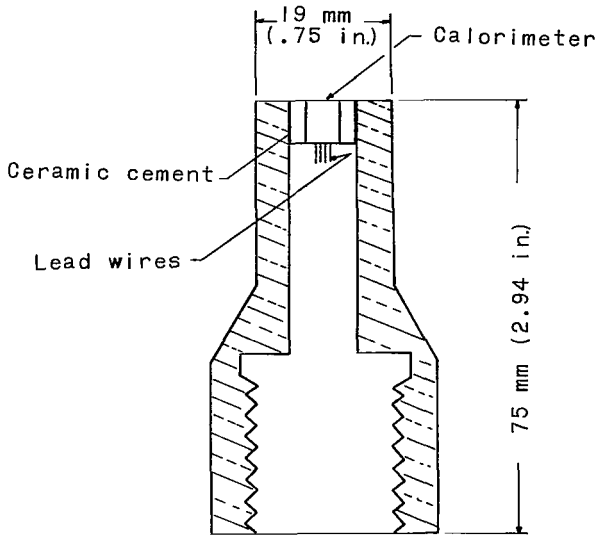

(b) Detail shown in cross section.

Figure 8.- Concluded.

as compared with the diameter of the calorimeter to minimize the variation of heating rate across the front surface in the radial direction.

The details of the thermocouple installation are shown in figure 9. A nickel cylinder had grooves machined up the sides to the depth required for each thermocouple. The bead of a chromel-alumel thermocouple was peened in place at the depths tabulated in figure 9. A 25-μm (0.001-in.) wire covered with a thin quartz sleeve was used as a lead down the slot and to the back of the cylinder. At this point, a 76-μm (0.003-in.) wire was spliced to the 25-μm (0.001-in.) wire and extended about 2.5 cm (1 in.) from the back surface. After the thermocouples were installed, a nickel sleeve was fitted around the nickel cylinder and the junctions at the back surface were encapsulated. The 76-μm (0.003-in.) wires were then spliced to a 250-μm (0.01-in.) wire for which the leads were 2 m (7 ft) long.

Procedure

The nickel calorimeter was subjected to a heat pulse in an arc-heated air jet. This jet, described in reference 10, was fitted with a supersonic nozzle. The heating rate to a flat-faced cylinder of 19-mm (0.75-in.) diameter was determined from a number of measurements with thin calorimeters taken as described in reference 11. The heating rate determined by these measurements, taken when the calorimeter was fully inserted

into the air stream, was 4.52 MW/m^2 (398 Btu/ft^2-sec) ±4 percent. The thick calorimeter was inserted into the arc-heated air stream for approximately 1.5 seconds. A switch actuated by the sting was used to determine when the calorimeter was fully inserted into the air stream. The switch indicated that the total time required to insert the calorimeter into the air stream was 0.25 second. The thermocouple outputs were recorded by the Langley central digital data recording facility at a rate of 40 times per second.

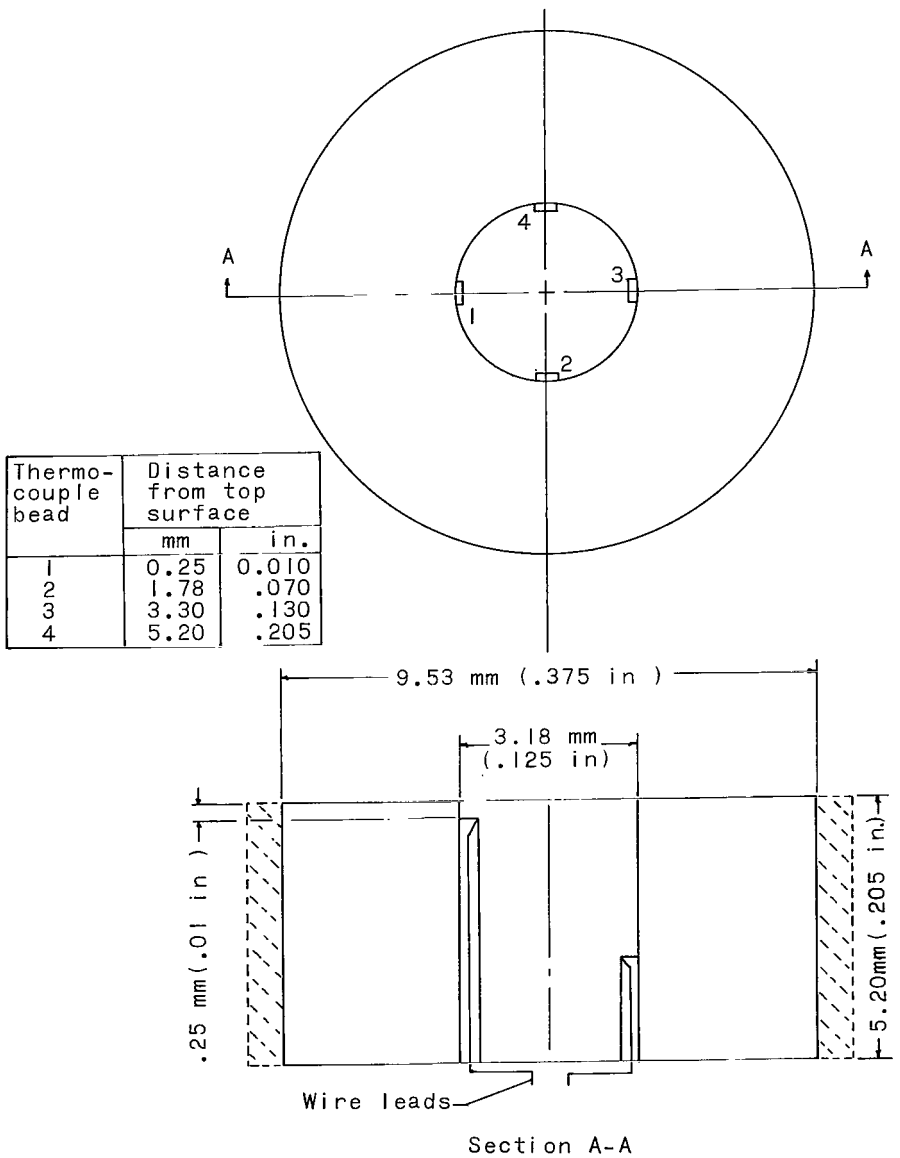

Thermocouple bead	Distance from top surface	
	mm	in.
1	0.25	0.010
2	1.78	.070
3	3.30	.130
4	5.20	.205

Figure 9.- Details of thermocouple location.

Experimental Results

An examination of the calorimeter after test showed virtually no recession of the holder. Therefore no change in heating rate should have occurred as a result of a shape change in the calorimeter assembly during the test.

Approximately 50 data points were obtained from each thermocouple during the test. These points were fitted with a fifth-degree least squares polynomial. This polynomial provided an efficient method of generating the temperature of the boundaries at any time and had the added advantage of eliminating some of the random noise superimposed on the thermocouple signal.

Figure 10 shows plots of the least squares polynomial obtained from the thermocouple data. The thermocouples are numbered as shown in figure 9. These curves agree with the data within 1 percent.

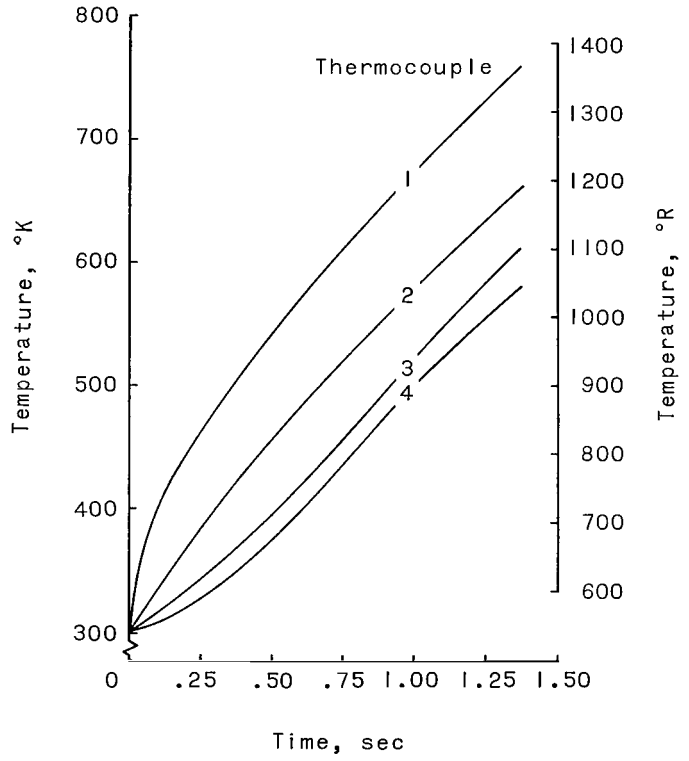

Figure 10.- Temperature response of thermocouples located in the calorimeter.

COMPARISON OF CALCULATED AND EXPERIMENTAL RESULTS

The experimental temperature histories of thermocouples (1) and (4), for which positions are shown in figure 9, were used as inputs to the thick calorimeter program. The material properties used in the program were taken from the most probable curves for nickel in reference 9.

The computed heating-rate history is shown in figure 11. The shaded band represents the range of steady state heating rate computed from thin calorimeter measurements made at discrete times in this facility. The solid line is the heating-rate history computed by the thick calorimeter program. The initial peak occurs when the thick calorimeter is inserted into the stream. This peak in heating rate has been observed previously when other calorimetric devices were used, and thus its existence for this experiment seems reasonable. The reason for this peak is not understood but may be caused by the large velocity gradients in the shear layer between the stream and the quiescent air. The termination of the specimen insertion cycle was recorded and occurred at 0.25 second during this test. The heating rate is nominally constant after the calorimeter is fully inserted into the stream. The heating rate determined by the thick calorimeter program fluctuates with time. Instantaneous results obtained with thin calorimeters were found to vary as much as 8 percent. Consequently, real fluctuations

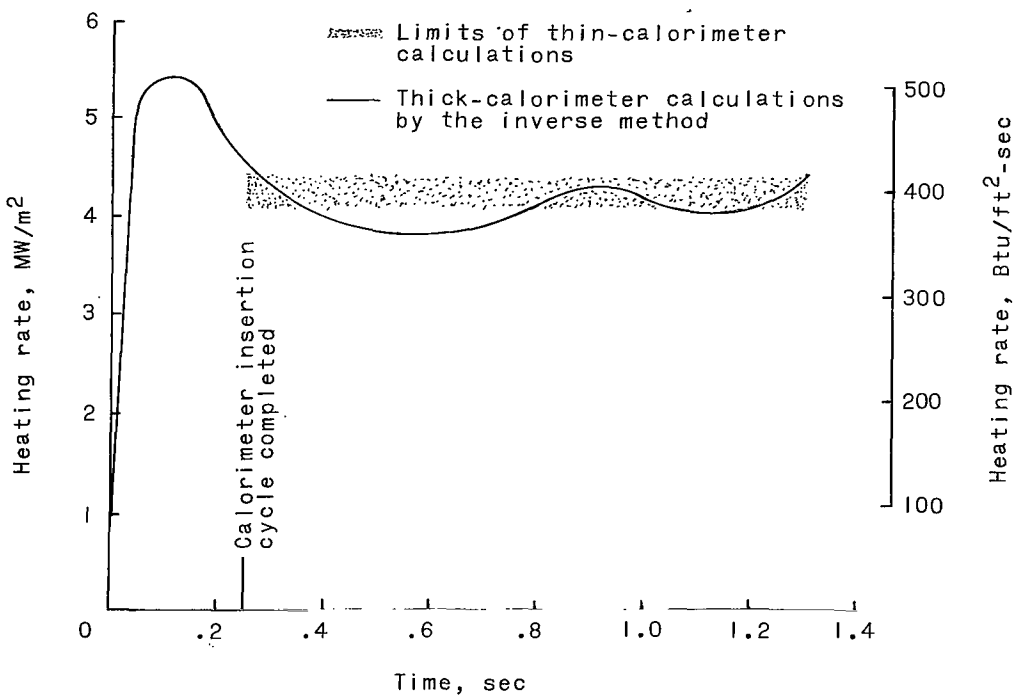

Figure 11.- Comparison of experimentally determined heating rates.

in heating rate may actually occur. As seen in figure 11, there is reasonable agreement between the thick and thin calorimeter calculations after the insertion cycle is complete. The maximum difference between calculated heating rates from the thick calorimeter and the bounds which occurred when thin calorimeters were used was 5.7 percent.

Table III shows the extrapolated front-surface temperatures and a comparison of measured and calculated internal temperatures. The difference between the measured and calculated results reflect not only the errors in the analytical procedure but also error associated with experimental procedures. These experimental errors include at least the following:

(1) Error in location of the thermocouple

(2) Calibration errors in the thermocouple wires

(3) Error in material property values for calorimeter material

(4) Lateral conduction effects

(5) Disturbance of the temperature field caused by the placement of the thermocouple

(6) Random noise induced in the thermocouple circuit by electromagnetic radiation

TABLE III.- COMPARISON OF CALCULATED AND MEASURED TEMPERATURES

Time, sec	Temperature at front surface		Temperature at station 2				Temperature at station 3			
			Measured		Calculated		Measured		Calculated	
	^{o}K	^{o}R	^{o}K	^{o}R	^{o}K	^{o}R	^{o}K	^{o}R	^{o}K	^{o}R
0	300	540	300	540	300	540	300	540	300	540
.25	464	836	372	670	371	668	342	615	340	612
.50	525	946	428	770	433	779	382	688	385	694
.75	585	1054	480	865	479	863	430	775	428	771
1.00	646	1163	536	965	532	957	480	865	478	860
1.25	699	1258	592	1065	584	1051	533	960	525	945

The error in location of the thermocouple is a function of thermocouple wire diameter, since it is not possible to locate the junction any more precisely than one wire diameter. The diameter of the wire used in the calorimeter tested was approximately 25 μm (0.001 inch). This diameter probably represents the lower limit on wire size and therefore determines the degree of precision attainable in thermocouple location. The errors caused by items (2), (3), and (4) in the preceding list can be reduced by careful

experimental technique. The disturbance caused by placement of the thermocouple is a function of the size of the hole drilled in the calorimeter for placement of the thermocouple. This item is not an important source of error in metals of high thermal conductivity.

The alternating currents in the arc-jet places the calorimeter in an electromagnetic radiation environment that is far more severe than any that is likely to be encountered in flight testing. This source of error was present in the experiment but did not appear to be large.

CONCLUDING REMARKS

A method has been presented for reducing the data obtained from a thick calorimeter to determine the heating rate to the surface of the calorimeter. The technique employed was to use a digital computer to obtain a numerical solution to the inverse problem of heat transfer. Comparisons were made with direct solutions and reasonable agreement was obtained. Experimental results were obtained and comparisons made between calculations using the inverse technique and calculations made from thin calorimeter measurements.

The data required to make these inverse calculations are the temperature histories of two points within the material, the initial temperature distribution through the calorimeter, and material property data as a function of temperature. Evaluation of the accuracy of the results obtained shows that a satisfactory determination of heating rates can be made with this method.

Langley Research Center,
National Aeronautics and Space Administration,
Langley Station, Hampton, Va., October 19, 1966,
124-08-03-25-23.

APPENDIX A

CONVERSION OF U.S. CUSTOMARY UNITS TO SI UNITS

The International System of Units (SI) was adopted by the Eleventh General Conference on Weights and Measures, Paris, October 1960, in resolution No. 12 (ref. 3). Conversion factors for the units used herein are given in the following table:

Physical quantity	U.S. Customary Unit	Conversion factor (*)	SI Unit
Heating rate	Btu/ft^2-sec	1.135×10^4	W/m^2
Length	ft	0.3048	m
	in.	0.0254	m
Temperature	^oR	5/9	^oK
Thermal conductivity	$Btu/ft-sec-^oR$	6226	$W/m-^oK$
Volumetric specific heat	Btu/ft^3-^oR	6.85×10^4	J/m^3-^oK

*Multiply value given in U.S. Customary Unit by conversion factor to obtain equivalent value in SI Unit.

Prefixes to indicate multiple of units are as follows:

Prefix	Multiple
mega (M)	10^6
centi (c)	10^{-2}
milli (m)	10^{-3}
micro (μ)	10^{-6}
nano (n)	10^{-9}

REFERENCES

1. Hill, P. R.: A Method of Computing the Transient Temperature of Thick Walls From Arbitrary Variation of Adiabatic-Wall Temperature and Heat-Transfer Coefficient. NACA Rept. 1372, 1958. (Supersedes NACA TN 4105.)

2. Brooks, William A., Jr.: Temperature and Thermal-Stress Distributions in Some Structural Elements Heated at a Constant Rate. NACA TN 4306, 1958.

3. Mechtly, E. A.: The International System of Units – Physical Constants and Conversion Factors. NASA SP-7012, 1964.

4. Carslaw, H. S.; and Jaeger, J. C.: Conduction of Heat in Solids. First ed., The Clarendon Press (Oxford), 1947.

5. Fourier, Joseph (Alexander Freeman, trans.): Theory of Heat. Great Books of the Western World, Vol. 45, Robert Maynard Hutchins, ed., Encyclopaedia Britannica, Inc., c.1952, pp. 163-251.

6. Richtmyer, Robert D.: Difference Methods in Initial-Value Problems. Interscience Pub., Inc., 1957.

7. Hildebrand, F. B.: On the Convergence of Numerical Solutions of the Heat-Flow Equation. J. Math. Phys., vol. 31, 1952, pp. 35-41.

8. Swann, Robert T.; and Pittman, Claud M.: Numerical Analysis of the Transient Response of Advanced Thermal Protection Systems for Atmospheric Entry. NASA TN D-1370, 1962.

9. Goldsmith, Alexander; Waterman, Thomas E.; and Hirschhorn, Harry T.: Thermophysical Properties of Solid Materials. Volume I: Elements. Rev. ed., The Macmillan Co., 1961.

10. Brown, Ronald D.; and Levin, L. Ross: A 6-Inch Subsonic High-Temperature Arc Tunnel for Structures and Materials Tests. NASA TN D-1621, 1963.

11. Brown, Ronald D.: A Comparison of the Theoretical and Experimental Stagnation-Point Heat Transfer in an Arc-Heated Subsonic Stream. NASA TN D-1927, 1964.

"The aeronautical and space activities of the United States shall be conducted so as to contribute . . . to the expansion of human knowledge of phenomena in the atmosphere and space. The Administration shall provide for the widest practicable and appropriate dissemination of information concerning its activities and the results thereof."

—NATIONAL AERONAUTICS AND SPACE ACT OF 1958

NASA SCIENTIFIC AND TECHNICAL PUBLICATIONS

TECHNICAL REPORTS: Scientific and technical information considered important, complete, and a lasting contribution to existing knowledge.

TECHNICAL NOTES: Information less broad in scope but nevertheless of importance as a contribution to existing knowledge.

TECHNICAL MEMORANDUMS: Information receiving limited distribution because of preliminary data, security classification, or other reasons.

CONTRACTOR REPORTS: Technical information generated in connection with a NASA contract or grant and released under NASA auspices.

TECHNICAL TRANSLATIONS: Information published in a foreign language considered to merit NASA distribution in English.

TECHNICAL REPRINTS: Information derived from NASA activities and initially published in the form of journal articles.

SPECIAL PUBLICATIONS: Information derived from or of value to NASA activities but not necessarily reporting the results of individual NASA-programmed scientific efforts. Publications include conference proceedings, monographs, data compilations, handbooks, sourcebooks, and special bibliographies.

Details on the availability of these publications may be obtained from:

SCIENTIFIC AND TECHNICAL INFORMATION DIVISION

NATIONAL AERONAUTICS AND SPACE ADMINISTRATION

Washington, D.C. 20546